crystals

MDPI

Article

Is Reduced Strontium Titanate a Semiconductor or a Metal?

Christian Rodenbücher [1,*], Christo Guguschev [2], Carsten Korte [1], Sebastian Bette [3] and Kristof Szot [3,4]

1 Institute of Energy and Climate Research (IEK-14), Forschungszentrum Jülich GmbH, 52425 Jülich, Germany; c.korte@fz-juelich.de
2 Leibniz-Institut für Kristallzüchtung (IKZ), 12489 Berlin, Germany; christo.guguschev@ikz-berlin.de
3 aixACCT Systems GmbH, 52068 Aachen, Germany; bette@aixacct.com (S.B.); krzysztof.szot@us.edu.pl (K.S.)
4 A. Chełkowski Institute of Physics, University of Silesia, 41-500 Chorzów, Poland
* Correspondence: c.rodenbuecher@fz-juelich.de

Abstract: In recent decades, the behavior of $SrTiO_3$ upon annealing in reducing conditions has been under intense academic scrutiny. Classically, its conductivity can be described using point defect chemistry and predicting n-type or p-type semiconducting behavior depending on oxygen activity. In contrast, many examples of metallic behavior induced by thermal reduction have recently appeared in the literature, challenging this established understanding. In this study, we aim to resolve this contradiction by demonstrating that an initially insulating, as-received $SrTiO_3$ single crystal can indeed be reduced to a metallic state, and is even stable against room temperature reoxidation. However, once the sample has been oxidized at a high temperature, subsequent reduction can no longer be used to induce metallic behavior, but semiconducting behavior in agreement with the predictions of point defect chemistry is observed. Our results indicate that the dislocation-rich surface layer plays a decisive role and that its local chemical composition can be changed depending on annealing conditions. This reveals that the prediction of the macroscopic electronic properties of $SrTiO_3$ is a highly complex task, and not only the current temperature and oxygen activity but also the redox history play an important role.

Keywords: strontium titanate; thermal reduction; insulator–metal transition; redox reactions; point defect chemistry

Citation: Rodenbücher, C.; Guguschev, C.; Korte, C.; Bette, S.; Szot, K. Is Reduced Strontium Titanate a Semiconductor or a Metal? *Crystals* **2021**, *11*, 744. https://doi.org/10.3390/cryst11070744

Academic Editor: Giuseppe Greco

Received: 31 May 2021
Accepted: 23 June 2021
Published: 25 June 2021

1. Introduction

Redox processes in transition metal oxides have been under investigations for decades, given their substantial potential for applications in the fields of sensorics, information technology, superconductivity, and energy conversion [1–5]. $SrTiO_3$ has emerged as one of the most widely investigated model materials for metal oxides with a perovskite structure and its electronic properties have been intensively analyzed [6,7]. Although stoichiometric $SrTiO_3$ is an insulator, it can be turned into a semiconductor by means of doping with extrinsic donors or self-doping with oxygen vacancies [8]. The redox behavior of $SrTiO_3$ has been described in theoretical terms using point defect chemistry [9–11]. As the dominant type of disorder in $SrTiO_3$ is of the Schottky variety, the properties of the surface/surface layer play a key role in exchange processes. By using the equilibrium constants of the partial reactions between the relevant point defects in combination with the charge neutrality condition, the conductivity of $SrTiO_3$ can be calculated as a function of the surrounding oxygen partial pressure at sufficiently high temperatures. It is predicted that in a regime with a high oxygen partial pressure, $SrTiO_3$ behaves as a p-type semiconductor, whereas n-type conductivity prevails under reducing conditions [12]. This behavior has been experimentally confirmed using ceramics and single crystals of $SrTiO_3$ in many studies over the last 30 years [9,11,13–16].

However, for $SrTiO_3$ single crystals, which were annealed under vacuum conditions (at an oxygen partial pressure in the range of 10^{-9} mbar), a completely different behavioral pattern has been observed. During the annealing process, an insulator–metal transition

occurs, boosting the macroscopic conductivity of $SrTiO_3$ into regions far beyond those predicted by point defect chemistry [17]. Even more surprisingly, the transition into the metallic state was found to take place upon the effusion of an extremely small amount of oxygen, in the range of $10^{13}/cm^3$, from the $SrTiO_3$ crystal [18]. As each oxygen atom removed from the lattice leaves behind a two-fold positively charged vacancy being compensated by electrons, it can be assumed that the concentration of electrons in the oxide is equal to the effused oxygen. Hence, at an extremely low carrier concentration, the crystal would be metallic, which stands in conflict with the Mott criterion that predicts metallicity only at concentrations above $10^{18}/cm^3$ [19]. As an explanation for this discrepancy, it must be assumed that the metallic behavior of reduced $SrTiO_3$ single crystals is caused by a local phenomenon. Indeed, it has been found that this metallic conductivity is confined to a region close to the surface and, under certain conditions, even 2D electron gases at the surface have been identified [20–23]. Furthermore, it has been considered that the surface layer of real crystals has a high concentration of dislocations, which constitute preferential reduction sites [24–26]. Dislocations are intrinsically present in Czochralski grown crystals with a density of about $10^6/cm^2$ [27]. Upon cutting and polishing, further dislocations are introduced into the surface layer, reaching local densities above $10^9/cm^2$ [28]. Thus, the Mott criterion could be fulfilled in regions close to the reduced dislocations, leading to the evolution of metallic filaments within an insulating matrix. This effect could also be exploited for resistive switching applications [29]. Using experimental methods with a high spatial resolution, such as optical imaging, in combination with local conductivity atomic force microscopy (LC-AFM), it has been proven that dislocations in $SrTiO_3$ serve as a template for the formation of metallic filaments upon thermal reduction, thus leading to a preferential reduction in the dislocation-rich surface region [28,30].

In this study, we aim to discuss the conditions under which either metallic or point defect chemistry-like behavior can be observed. Therefore, we perform annealing experiments on an $SrTiO_3$ single crystal while simultaneously measuring the sample resistance using a four probe setup. Repeating the heating and cooling cycles on the same sample but under different oxygen pressures allows a linking of the electrical properties with its redox history.

2. Materials and Methods

Nominally undoped $SrTiO_3$ single crystals were prepared following the Czochralski method and using starting powders of 99.99% purity [27]. Samples of the crystal with dimensions of 10 mm × 4 mm × 1 mm were cut out of the crystal boule in (100) direction and the surface was mechanically polished.

The redox behavior of the sample was analyzed by an aixDCA setup (aixACCT Systems, Aachen, Germany). Four electrodes covering both sides of the samples were deposited by Pt paste, as is illustrated in Figure 1a. The electrodes were wrapped with Pt wires, thus establishing an electrical connection to the measurement system. A small alternating voltage (4 mV, 172.5 Hz) was applied via the two outer electrodes. Using a lock-in technique, the current through the sample and the potentials at the four electrodes were measured. The use of a four probe setup allows determining not only the total resistance, but also the partial resistances. The nearly current free measurement of the potential drop between the inner electrodes can be used to determine the bulk resistance, while the potential drops between inner and outer electrodes on each side (I and II) are related to the interface resistance, which is mainly determined by the resistance of the surface layer [31]. As is described in detail elsewhere [11], the sample was placed in a quartz tube furnace connected to an ultrahigh vacuum pumping system. The oxygen activity was controlled by filling pure oxygen into the vacuum chamber.

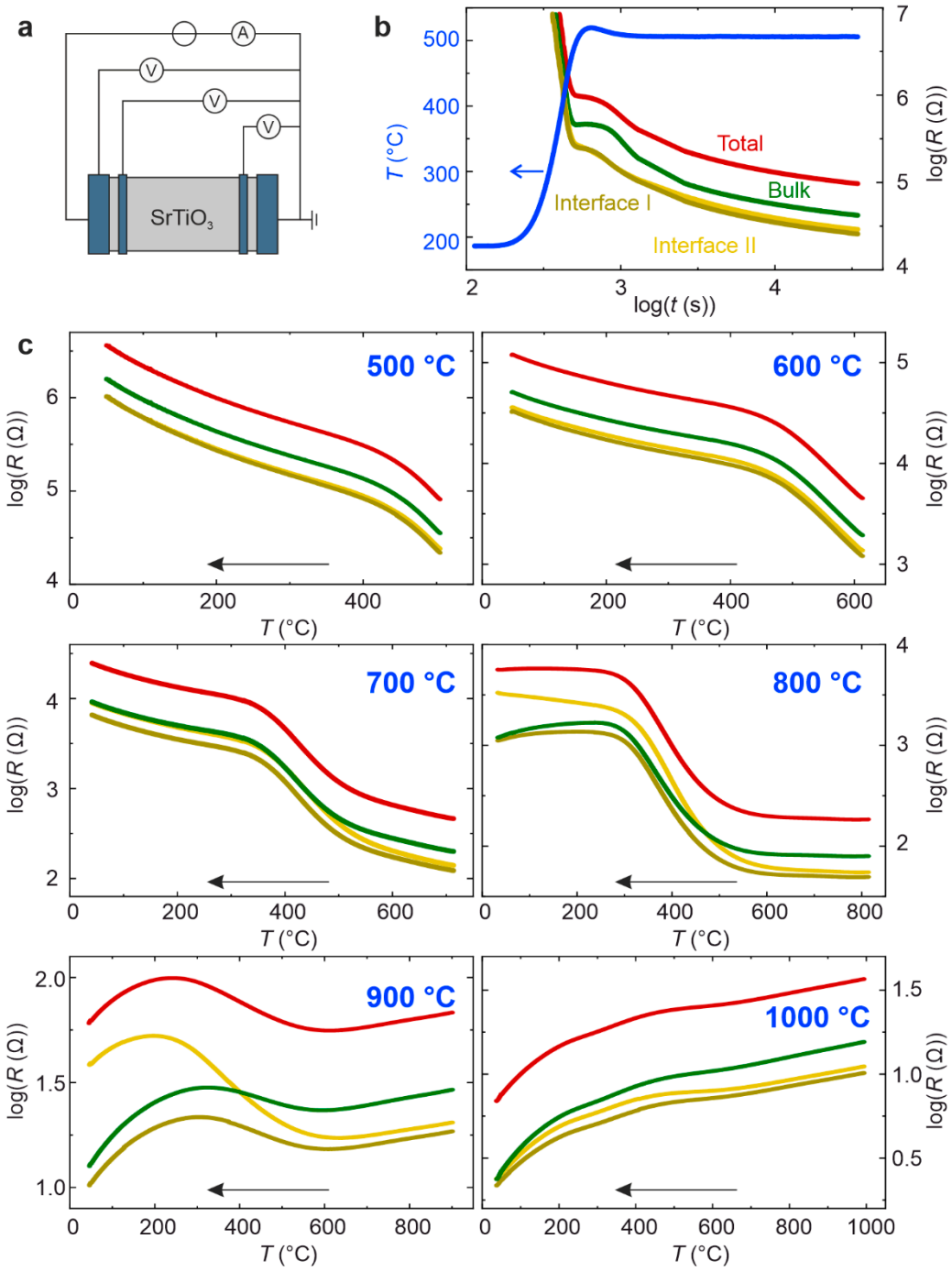

Figure 1. Four probe resistance measurements of the $SrTiO_3$ single crystal: (**a**) schematic setup; (**b**) total and partial resistances of the sample during the first heating to 500 °C; (**c**) cooling curves of the resistances after thermal reduction at increasing maximum temperatures.

3. Results

After the chamber had been baked at 200 °C with the freshly prepared sample under vacuum conditions to reduce the amount of physisorbed species, the resistance of the sample was still above the measurement limit of the used setup (>10^8 Ω), indicating insulating behavior. During the first heating cycle, from 200 to 500 °C, the resistance dropped by many orders of magnitude, converging on a total resistance of around 10^5 Ω, as is depicted in Figure 1b. The partial resistances of the bulk and the two interfaces, which were simultaneously measured by the four probe technique, followed the same trend and decreased as a function of the temperature. The bulk resistance was higher than the

surface/interface resistances. The temperature of the chamber was held at 500 °C for 9 h before being cooled to room temperature. Upon cooling, the resistance increased again but reached a value of 3.6 MΩ, which is significantly lower than the initial resistance, indicating that the sample had been reduced and self-doped under vacuum conditions (Figure 1c). This scheme of annealing and cooling cycles under vacuum conditions was repeated for different temperatures in steps of 100 °C until the maximum annealing temperature of 1000 °C was reached.

Figure 1c displays the resistance curves obtained during cooling from the respective annealing temperatures. In general, the resistance decreased continuously during annealing as an effect of the ongoing reduction via the removal of oxygen from the crystal. After annealing to 500, 600 and 700 °C, the cooling curves reveal an increase in the resistance with decreasing temperature, which is typical for a thermally activated semiconductor. At 800 °C, the total resistance still increased with decreasing temperature, but the bulk resistance reached a maximum and then decreased again upon further cooling, whereas the resistance of interface II continued to increase. After annealing at 900 °C, the resistance initially decreased upon cooling until approximately 600 °C, and then increased again to reach a maximum around approximately 250 °C, before it strongly decreased until reaching room temperature. Moreover, in this measurement, the resistance of interface II at low temperatures was higher than that of the bulk and of interface I, revealing that the sample had heterogeneous properties. After annealing at 1000 °C, the resistance continuously decreased upon cooling and the total resistance was more than six orders of magnitude smaller than that in the as-received state. This indicates that upon reduction, the crystal underwent an insulator–metal transition.

In the next step, we analyzed the impact of reoxidation on the self-doped crystal. To achieve this, we exposed the metallic sample to 200 mbar of pure O_2 at room temperature for four hours before evacuating the chamber again. As can be seen in Figure 2a, the resistance was virtually unaffected by the oxygen exposure and remained at the low level of a few ohms. Subsequently, we heated the crystal to 1000 °C under vacuum conditions with an oxygen partial pressure of approximately 10^{-9} mbar. The heating curve displayed in Figure 2b shows an increasing resistance, with the increasing temperature still indicating metallic behavior. At 1000 °C, the oxygen pressure was then raised to 3×10^{-7} mbar and the resistance was monitored as a function of the time. Figure 2c shows that the total resistance, as well as the partial resistances, increased upon high temperature oxygen exposure by more than three orders of magnitude. After 42 h, a near equilibrium state had been achieved, whereupon the sample was cooled down with a slightly increased oxygen pressure maintained. The cooling curve in Figure 2d reveals an increasing resistance with decreasing temperature, and shows that the sample had lost its metallicity and turned into a semiconducting or insulating state. At room temperature, the resistance was above the measurement limit, similar to the samples in the as-received state. Subsequently, the temperature was increased to 1000 °C and the chamber held under vacuum conditions. As is shown in Figure 3a, the resistance measured during heating exhibited semiconducting properties. The sample did not return to a metallic state. While the temperature was being held at 1000 °C, the oxygen pressure was increased in different steps, up to a final pressure of 200 mbar (Figure 3b). Before starting each step, the resistance was monitored until near equilibrium conditions were achieved, as per the procedure previously described [11]. The bulk resistance measured in (near) equilibrium was used to calculate the macroscopic conductivity σ, which is displayed in Figure 3c as a function of the oxygen partial pressure. The same type of measurement was performed at 800 and 900 °C, resulting in a typical Brouwer diagram for $SrTiO_3$. This illustrates that the sample had been transformed into a semiconducting state, exhibiting a temperature and oxygen partial pressure dependence, which is in qualitative and quantitative agreement with the predictions of point defect chemistry and also with our previous experimental investigations of Verneuil grown $SrTiO_3$ (Figure 3d).

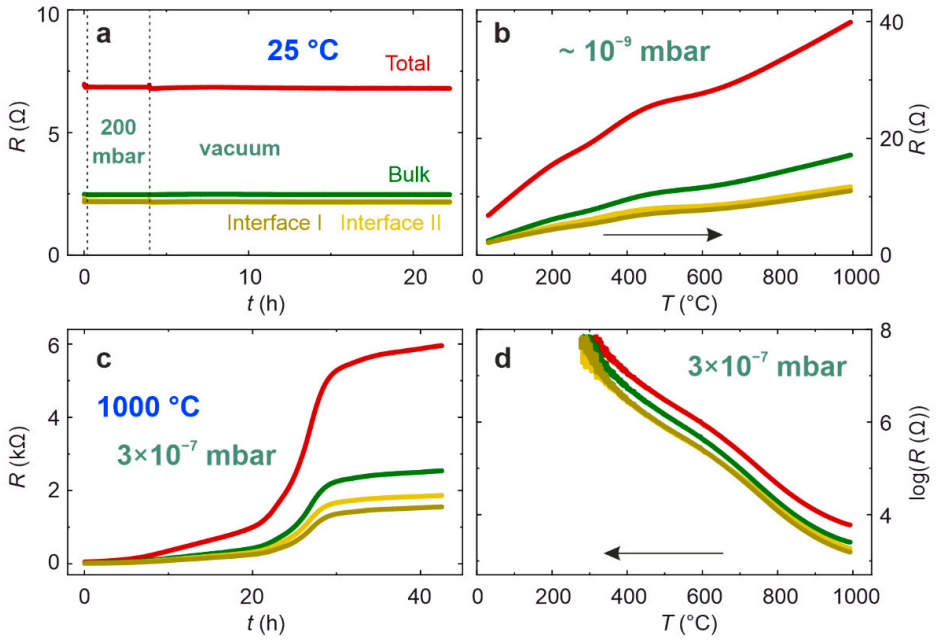

Figure 2. Resistance of the crystal during exposure to oxygen: (**a**) exposure to 200 mbar O_2 at room temperature for 4 h and subsequent re-evacuation; (**b**) heating to 1000 °C under vacuum conditions; (**c**) exposure to 3 × 10^{-7} mbar O_2 at 1000 °C; and (**d**) subsequent cooling at 3 × 10^{-7} mbar O_2.

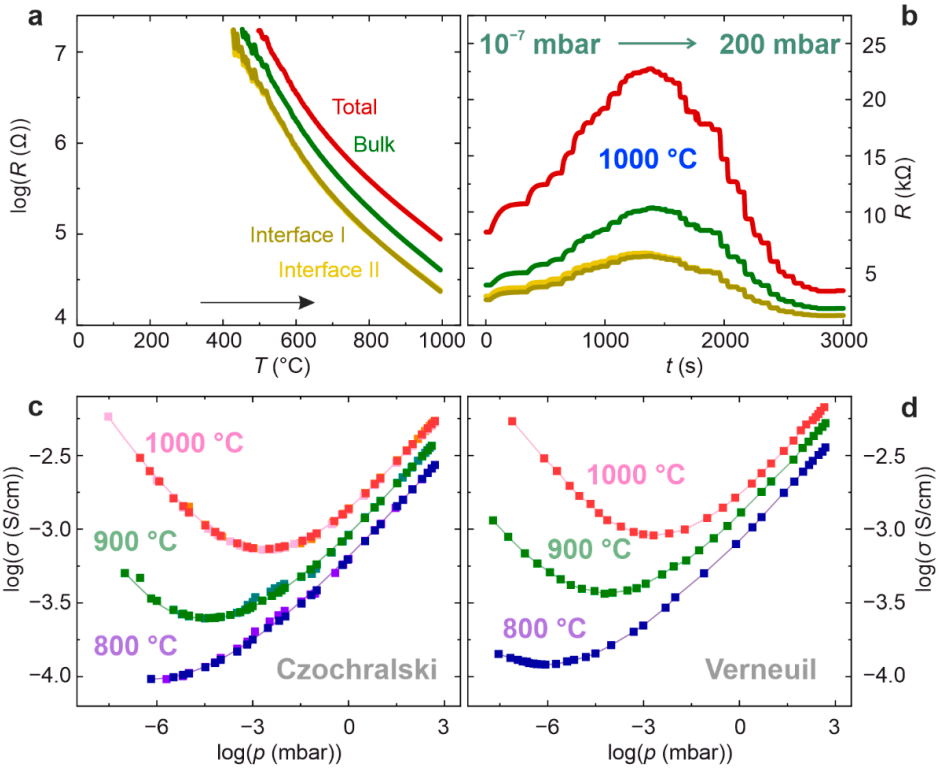

Figure 3. (**a**) Resistance during reannealing to 1000 °C under vacuum conditions following previous oxidation; (**b**) step-wise exposure to oxygen at 1000 °C; (**c**) Brouwer diagram of the macroscopic conductivity measured at different temperatures by step-wise oxidation (the differently toned data points indicate repeated measurement runs); and (**d**) Brower diagram measured on Verneuil grown $SrTiO_3$ for comparison [11].

Figure 4 summarizes the annealing experiments performed on the $SrTiO_3$ sample under investigation. It depicts the bulk resistance measured during cooling at the respective annealing temperatures. The curves labeled with 1–6 are the same as in Figure 1c and

reveal that the resistance decreased with increasing reduction temperature until finally a metallic behavior was present. After oxidation at a low oxygen pressure, the resistance jumped to a high value and the semiconducting properties were present (curve 7). Repeated annealing to 1000 °C under vacuum conditions slightly decreased the resistance at first, but, eventually, a stable semiconducting behavior was reached (curves 8–9).

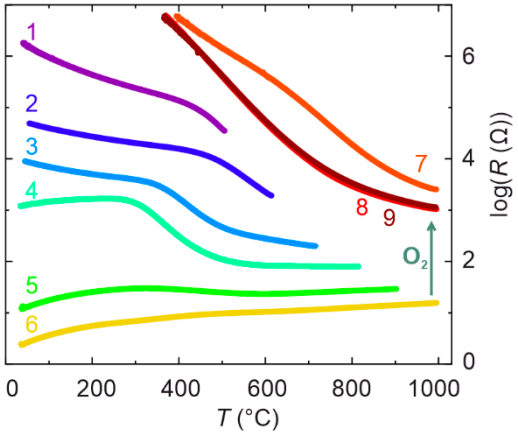

Figure 4. Overview of the measured bulk resistances obtained during cooling under vacuum conditions. The numbers indicate the sequence of the measurements.

4. Discussion

Our results reveal that $SrTiO_3$ single crystals can be transformed from an initially insulating state into a metallic one by means of thermal reduction under vacuum conditions at a temperature of 1000 °C. However, once a crystal has been exposed to a small amount of oxygen at high temperatures, it adopts a semiconducting state and does not return to the metallic one anymore, even after prolonged exposure to reducing vacuum conditions at 1000 °C. While the semiconducting state, obtained after exposure to oxygen, can be described by defect chemistry, the macroscopic conductivity of the metallic state would be far beyond theoretical predictions. In our view, this contradiction could be resolved by taking the special role of a region close to the surface of the $SrTiO_3$ single crystals into account, to which an increased density of nonequilibrium (2-D) defects, e.g., dislocations, can be attributed. As has been shown by four probe measurements, the metallic state is associated with the formation of conducting paths on this surface layer of the crystal [22,31,32]. The correlation between dislocations and conducting paths has also been illustrated by microscopy methods such as LC-AFM, revealing that those paths form in the vicinity of dislocations, which can be easily reduced [28]. Furthermore, the vacuum reduced surface region was found to be Ti-rich, indicating that Sr diffused away from the surface towards the bulk upon annealing [31,33]. This has been confirmed by SIMS depth profiling showing a Sr depletion close to the surface and a Sr enrichment in the subsurface region of reduced $SrTiO_3$ [34]. During this process, a complex defect structure could also develop with Ti_{Sr} antisite defects coupled to oxygen vacancies, or the formation of TiO_x nanophases [35,36]. Hence, a heterogeneous surface layer is generated that is depleted in Sr but enriched in oxygen vacancies featuring a filamentary metallic conductivity. Upon high temperature reduction, even the crystallographic structure close to the dislocations themselves could change towards that of Ti suboxides, thus building up a metallic structure resistant to room temperature oxidation [37,38]. Upon high temperature oxidation, the opposite effects will occur. The surface oxygen vacancies will be filled and Sr will move towards the surface, eventually forming an SrO terminated surface or even SrO nanocrystals [39,40]. It should be noted that the reoxidation depends subtly on the chemical composition of the material, and it has been reported that specially prepared crystals can remain reduced, even after high temperature oxidation [41]. As extended defects such as dislocations and antiphase boundaries could provide easy diffusion paths for Sr, the stoichiometry and

crystallographic structure of the dislocations themselves might also be altered [42,43]. The segregation of the Sr to the surface might also have impact on the oxygen exchange kinetics, as an SrO termination was found to inhibit the efficient formation of oxygen vacancies upon exposure to reducing conditions [44]. Hence, once a Sr enriched surface has been generated by annealing under oxidizing conditions, the oxygen exchange could only allow for an equilibration of the oxygen vacancy concentration of the crystal according to point defect chemistry, but not for the generation of excess oxygen vacancies at the surface and close to dislocations, as this would be needed for metallic conductivity. This scenario can be supported by the measurements of the effusion of oxygen from the reoxidized $SrTiO_3$ crystals, which show comparable concentrations of removed oxygen atoms to those from virgin crystals, although the metallicity in the surface region cannot be generated [45]. This could indicate that the galvanic connections of the metallic filaments formed close to the dislocation cores have been disrupted by an insulating fragment with SrO enrichment.

5. Conclusions

In summary, we have shown that one and the same $SrTiO_3$ sample can be transformed into either a state associated with metallic behavior or to a state of semiconducting behavior that can be described by point defect chemistry through exposure to reducing conditions. The difference between these two results is a high temperature oxidation step, which must be performed beforehand in order to attain the semiconducting properties. Otherwise, metallic surface conductivity arises. We have discussed the fact that changes in the chemical composition in the dislocation-rich surface layer may irreversibly modify the sample, such that once oxidized, the sample can no longer be brought into the metallic state. Hence, the question of whether reduced $SrTiO_3$ would behave as a metal or semiconductor can only be answered if the redox history of the sample is known. This offers opportunities for designing the electronic properties of solid oxides by a well-thought-out sequence of annealing steps in oxidizing and reducing atmospheres.

Author Contributions: Conceptualization, investigation, formal analysis, and visualization, C.R. and K.S.; resources (crystal growth), C.G.; writing—original draft preparation, C.R.; validation and writing—review and editing, C.R., C.G., C.K., S.B. and K.S. All authors have read and agreed to the published version of the manuscript.

Funding: The work at IKZ was supported by a project of the Leibniz Association under reference number SAW-2013-IKZ-2.

Institutional Review Board Statement: Not applicable.

Informed Consent Statement: Not applicable.

Data Availability Statement: Data is contained within the article.

Acknowledgments: We gratefully acknowledge C. Wood for proofreading the manuscript.

Conflicts of Interest: The authors declare no conflict of interest.

References

1. Ielmini, D. Resistive switching memories based on metal oxides: Mechanisms, reliability and scaling. *Semicond. Sci. Technol.* **2016**, *31*, 063002. [CrossRef]
2. Szafraniak, B.; Fusnik, L.; Xu, J.; Gao, F.; Brudnik, A.; Rydosz, A. Semiconducting metal oxides: $SrTiO_3$, $BaTiO_3$ and $BaSrTiO_3$ in gas-sensing applications: A review. *Coatings* **2021**, *11*, 185. [CrossRef]
3. Verbraeken, M.C.; Ramos, T.; Agersted, K.; Ma, Q.; Savaniu, C.D.; Sudireddy, B.R.; Irvine, J.T.S.; Holtappels, P.; Tietz, F. Modified strontium titanates: From defect chemistry to SOFC anodes. *RSC Adv.* **2015**, *5*, 1168–1180. [CrossRef]
4. Rodenbücher, C.; Szot, K. Electronic phenomena of transition metal oxides. *Crystals* **2021**, *11*, 256. [CrossRef]
5. Bussmann-Holder, A.; Keller, H. From $SrTiO_3$ to cuprates and back to $SrTiO_3$: A way along Alex Müller's scientific career. *Condens. Matter* **2020**, *6*, 2. [CrossRef]
6. Aschauer, U.; Spaldin, N.A. Competition and cooperation between antiferrodistortive and ferroelectric instabilities in the model perovskite $SrTiO_3$. *J. Phys. Condens. Matter* **2014**, *26*, 122203. [CrossRef] [PubMed]

7. Merkle, R.; Maier, J. How is oxygen incorporated into oxides? A comprehensive kinetic study of a simple solid-state reaction with $SrTiO_3$ as a model material. *Angew. Chem. Int. Ed.* **2008**, *47*, 3874–3894. [CrossRef]
8. Spinelli, A.; Torija, M.A.; Liu, C.; Jan, C.; Leighton, C. Electronic transport in doped $SrTiO_3$: Conduction mechanisms and potential applications. *Phys. Rev. B* **2010**, *81*, 155110. [CrossRef]
9. Moos, R.; Härdtl, K.H. Defect chemistry of donor-doped and undoped strontium titanate ceramics between 1000° and 1400 °C. *J. Am. Ceram. Soc.* **1997**, *80*, 2549–2562. [CrossRef]
10. Denk, I.; Münch, W.; Maier, J. Partial conductivities in $SrTiO_3$: Bulk polarization experiments, oxygen concentration cell measurements, and defect-chemical modeling. *J. Am. Ceram. Soc.* **1995**, *78*, 3265–3272. [CrossRef]
11. Rodenbücher, C.; Korte, C.; Schmitz-Kempen, T.; Bette, S.; Szot, K. A physical method for investigating defect chemistry in solid metal oxides. *APL Mater.* **2021**, *9*, 011106. [CrossRef]
12. Moos, R.; Hardtl, K.H. Dependence of the intrinsic conductivity minimum of $SrTiO_3$ ceramics on the sintering atmosphere. *J. Am. Ceram. Soc.* **1995**, *78*, 2569–2571. [CrossRef]
13. Ohly, C.; Hoffmann-Eifert, S.; Szot, K.; Waser, R. Electrical conductivity and segregation effects of doped $SrTiO_3$ thin films. *J. Eur. Ceram. Soc.* **2001**, *21*, 1673–1676. [CrossRef]
14. Menesklou, W.; Schreiner, H.-J.; Härdtl, K.H.; Ivers-Tiffée, E. High temperature oxygen sensors based on doped $SrTiO_3$. *Sens. Actuators B Chem.* **1999**, *59*, 184–189. [CrossRef]
15. Chan, N.-H.; Sharma, R.K.; Smyth, D.M. Nonstoichiometry in $SrTiO_3$. *J. Electrochem. Soc.* **1981**, *128*, 1762. [CrossRef]
16. Zhang, X.-D.; Li, J.-J.; Guo, X. Oxygen pump based on stabilized zirconia. *Rev. Sci. Instrum.* **2015**, *86*, 115103. [CrossRef]
17. Szot, K.; Speier, W.; Carius, R.; Zastrow, U.; Beyer, W. Localized metallic conductivity and self-healing during thermal reduction of $SrTiO_3$. *Phys. Rev. Lett.* **2002**, *88*, 075508. [CrossRef] [PubMed]
18. Szot, K.; Rodenbücher, C.; Bihlmayer, G.; Speier, W.; Ishikawa, R.; Shibata, N.; Ikuhara, Y. Influence of dislocations in transition metal oxides on selected physical and chemical properties. *Crystals* **2018**, *8*, 241. [CrossRef]
19. Szot, K.; Rodenbücher, C. Insulator-metal transition associated with resistive switching in real $SrTiO_3$ and TiO_2 crystals. In Proceedings of the 2015 Joint IEEE International Symposium on the Applications of Ferroelectric (ISAF), International Symposium on Integrated Functionalities (ISIF), and Piezoelectric Force Microscopy Workshop (PFM), Singapore, 24–27 May 2015; pp. 143–146. [CrossRef]
20. Santander-Syro, A.F.; Copie, O.; Kondo, T.; Fortuna, F.; Pailhés, S.; Weht, R.; Qiu, X.G.; Bertran, F.; Nicolaou, A.; Taleb-Ibrahimi, A.; et al. Two-dimensional electron gas with universal subbands at the surface of $SrTiO_3$. *Nature* **2011**, *469*, 189–194. [CrossRef] [PubMed]
21. Cook, S.; Dylla, M.T.; Rosenberg, R.A.; Mansley, Z.R.; Snyder, G.J.; Marks, L.D.; Fong, D.D. The vacancy-induced electronic structure of the $SrTiO_{3-\delta}$ surface. *Adv. Electron. Mater.* **2019**, *5*, 1800460. [CrossRef]
22. Leis, A.; Rodenbücher, C.; Szot, K.; Cherepanov, V.; Tautz, F.S.; Voigtländer, B. In-situ four-tip STM investigation of the transition from 2D to 3D charge transport in $SrTiO_3$. *Sci. Rep.* **2019**, *9*, 2476. [CrossRef]
23. Sing, M.; Jeschke, H.O.; Lechermann, F.; Valenti, R.; Claessen, R. Influence of oxygen vacancies on two-dimensional electron systems at $SrTiO_3$-based interfaces and surfaces. *Eur. Phys. J. Spec. Top.* **2017**, *226*, 2457–2475. [CrossRef]
24. Marrocchelli, D.; Sun, L.; Yildiz, B. Dislocations in $SrTiO_3$: Easy to reduce but not so fast for oxygen transport. *J. Am. Chem. Soc.* **2015**, *137*, 4735–4748. [CrossRef] [PubMed]
25. Wang, P.; Yi, W.; Chen, J.; Ito, S.; Cui, C.; Sekiguchi, T. Oxygen vacancy migration along dislocations in $SrTiO_3$ studied by cathodoluminescence. *J. Phys. Appl. Phys.* **2019**, *52*, 475103. [CrossRef]
26. Wang, R.; Zhu, Y.; Shapiro, S.M. Structural defects and the origin of the second length scale in $SrTiO_3$. *Phys. Rev. Lett.* **1998**, *80*, 2370–2373. [CrossRef]
27. Guguschev, C.; Galazka, Z.; Kok, D.J.; Juda, U.; Kwasniewski, A.; Uecker, R. Growth of $SrTiO_3$ bulk single crystals using edge-defined film-fed growth and the Czochralski methods. *Crystengcomm* **2015**, *17*, 4662–4668. [CrossRef]
28. Rodenbücher, C.; Wrana, D.; Gensch, T.; Krok, F.; Korte, C.; Szot, K. The electronic properties of extended defects in $SrTiO_3$—A case study of a real bicrystal boundary. *Crystals* **2020**, *10*, 665. [CrossRef]
29. Szot, K.; Speier, W.; Bihlmayer, G.; Waser, R. Switching the electrical resistance of individual dislocations in single-crystalline $SrTiO_3$. *Nat. Mater.* **2006**, *5*, 312–320. [CrossRef]
30. Rodenbücher, C.; Bittkau, K.; Bihlmayer, G.; Wrana, D.; Gensch, T.; Korte, C.; Krok, F.; Szot, K. Mapping the conducting channels formed along extended defects in $SrTiO_3$ by means of scanning near-field optical microscopy. *Sci. Rep.* **2020**, *10*, 17763. [CrossRef] [PubMed]
31. Wrana, D.; Rodenbücher, C.; Bełza, W.; Szot, K.; Krok, F. In situ study of redox processes on the surface of $SrTiO_3$ single crystals. *Appl. Surf. Sci.* **2018**, *432*, 46–52. [CrossRef]
32. Bussmann-Holder, A.; Keller, H.; Simon, A.; Bihlmayer, G.; Roleder, K.; Szot, K. Unconventional co-existence of insulating nano-regions and conducting filaments in reduced $SrTiO_3$: Mode softening, local piezoelectricity, and metallicity. *Crystals* **2020**, *10*, 437. [CrossRef]
33. Szot, K.; Bihlmayer, G.; Speier, W. Nature of the resistive switching phenomena in TiO_2 and $SrTiO_3$. In *Solid State Physics 65*; Camley, R.E., Stamps, R.L., Eds.; Academic Press: Cambridge, MA, USA, 2014; pp. 353–559.
34. Szot, K.; Speier, W.; Herion, J.; Freiburg, C. Restructuring of the surface region in $SrTiO_3$. *Appl. Phys. Mater. Sci. Process.* **1996**, *64*, 55–59. [CrossRef]

35. Karjalainen, A.; Prozheeva, V.; Makkonen, I.; Guguschev, C.; Markurt, T.; Bickermann, M.; Tuomisto, F. Ti_{Sr} antisite: An abundant point defect in $SrTiO_3$. *J. Appl. Phys.* **2020**, *127*, 245702. [CrossRef]
36. Wrana, D.; Rodenbücher, C.; Jany, B.R.; Kryshtal, O.; Cempura, G.; Kruk, A.; Indyka, P.; Szot, K.; Krok, F. A bottom-up process of self-formation of highly conductive titanium oxide (TiO) nanowires on reduced $SrTiO_3$. *Nanoscale* **2019**, *11*, 89–97. [CrossRef] [PubMed]
37. Du, H.; Jia, C.-L.; Mayer, J. Local crystallographic shear structures in *a* [201] extended mixed dislocations of $SrTiO_3$ unraveled by atomic-scale imaging using transmission electron microscopy and spectroscopy. *Faraday Discuss.* **2019**, *213*, 245–258. [CrossRef]
38. Gao, P.; Ishikawa, R.; Feng, B.; Kumamoto, A.; Shibata, N.; Ikuhara, Y. Atomic-scale structure relaxation, chemistry and charge distribution of dislocation cores in $SrTiO_3$. *Ultramicroscopy* **2018**, *184*, 217–224. [CrossRef] [PubMed]
39. Szot, K.; Speier, W. Surfaces of reduced and oxidized $SrTiO_3$ from atomic force microscopy. *Phys. Rev. B* **1999**, *60*, 5909–5926. [CrossRef]
40. Huijbregtse, J.M.; Rector, J.H.; Dam, B. Effect of the two (100) $SrTiO_3$ substrate terminations on the nucleation and growth of $YBa_2Cu_3O_{7-\delta}$ thin films. *Phys. C Supercond.* **2001**, *351*, 183–199. [CrossRef]
41. Guguschev, C.; Kok, D.J.; Galazka, Z.; Klimm, D.; Uecker, R.; Bertram, R.; Naumann, M.; Juda, U.; Kwasniewski, A.; Bickermann, M. Influence of oxygen partial pressure on $SrTiO_3$ bulk crystal growth from non-stoichiometric melts. *CrystEngComm* **2015**, *17*, 3224–3234. [CrossRef]
42. Heisig, T.; Kler, J.; Du, H.; Baeumer, C.; Hensling, F.; Glöß, M.; Moors, M.; Locatelli, A.; Menteş, T.O.; Genuzio, F.; et al. Antiphase boundaries constitute fast cation diffusion paths in $SrTiO_3$ memristive devices. *Adv. Funct. Mater.* **2020**, 2004118. [CrossRef]
43. Gries, U.N.; Kessel, M.; Hensling, F.V.E.; Dittmann, R.; Martin, M.; De Souza, R.A. Behavior of cation vacancies in single-crystal and in thin-film $SrTiO_3$: The importance of strontium vacancies and their defect associates. *Phys. Rev. Mater.* **2020**, *4*, 123404. [CrossRef]
44. Hensling, F.V.E.; Baeumer, C.; Rose, M.-A.; Gunkel, F.; Dittmann, R. $SrTiO_3$ termination control: A method to tailor the oxygen exchange kinetics. *Mater. Res. Lett.* **2020**, *8*, 31–40. [CrossRef]
45. Szot, K. Nature of the chemical transformation of the surface layer of the prototypic ABO_3 perovskites. In Proceedings of the EMRS Fall Meeting, Warsaw, Poland, 19–22 September 2016.